NOTICE CONCERNING COPYRIGHT RESTRICTIONS

Modeling Fracture Initiation and Propagation Using A Poro-Thermoelastic Boundary Element Method

Q. Zhang and A. Ghassemi

Department of Geology and Geological Engineering
University of North Dakota, Grand Forks, ND

Keywords

Boundary element, hydraulic fracture, poroelasticity, thermoelasticity, wellbore failure.

ABSTRACT

The development of an indirect transient boundary element method (BEM) is described. The approach is formulated within the framework of non-isothermal poroelasticity and can be used to solve coupled porothermoelastic problems. The fundamental solutions and numerical procedures are described and some applications are presented. In particular, the model is used to study the stress and pore pressure distributions around a wellbore drilled in a hot rock. There is good agreement between the numerical predictions and analytical results. The analysis is useful for determining the conditions for wellbore failure while drilling as well as for calculating fracture initiation pressure for hydraulic fracturing.

Introduction

When rocks are heated/cooled, the bulk solid as well as the pore fluid tend to undergo expansion/contraction. A volumetric expansion can result in significant pressurization of the pore fluid depending on the degree of containment and the thermal and hydraulic properties of the fluid as well as the solid. The net effect is a coupling of thermal and poromechanical processes that plays an important role in many scientific and engineering activities related to production of geothermal resources.

The theory of poroelasticity couples pore pressure and solid stress fields in deformable fluid saturated porous rocks (Biot, 1941). In the isothermal poroelastic theory, the time dependent fluid flow is incorporated by combining the fluid mass conservation with Darcy's law; and the basic constitutive equations relate the total stress to both the effective stress given by deformation of the rock matrix and the pore pressure arising from the fluid. Meanwhile, in many geomechanics problems such as studies concerned with initiation and propagation of hydraulic fractures and borehole stability analysis in high-temperature rocks, thermally induced pore pressure and stresses also play an important role in rock deformation and fracture. A thermoelastic approach combines the theory of heat conduction with elastic constitutive equations coupling the temperature field with the stresses (Norris, 1992). In order to consider the influence of a temperature gradient on both pore pressure and stresses, it is necessary to use a non-isothermal poroelastic theory, or poro-thermoelasticity (Palciauskas and Domenico, 1982).

Governing Equations of Poro-Thermoelasticity

From the constitutive, balance, and transport laws, the governing equations of poro-thermoelasticity can be written as (Palciauskas and Domenico, 1982; Booker and Smith, 1993; Berchenko, 1998):

Navier Equation:

$$G\nabla^2 u_i + \frac{1}{3}(G+3K)\varepsilon_{,i} = \alpha p_{,i} + K\beta_s T_{,i} \tag{1}$$

Diffusion equation for pore pressure p:

$$\kappa\nabla^2 p = \frac{1}{M}\frac{\partial p}{\partial t} + b\frac{\partial \varepsilon}{\partial t} - \beta_m \frac{\partial T}{\partial t} \tag{2}$$

Diffusion equation for temperature T:

$$c^T \nabla^2 T = \frac{\partial T}{\partial t} \tag{3}$$

In the above equations, u_i denotes the solid displacement vector, ε_{ij} the total strain tensor, p the pore pressure, and T the temperature. The constants G, K, α, β_s, β_m, κ, M, and c^T represent shear modulus, drained bulk modulus of poroelastic matrix, Biot's poroelastic constant, drained thermal expansivity of the solid, thermal expansivity of the undrained saturated rock, mobility coefficient, Biot's modulus, and thermal diffusivity, respectively.

Biot's coefficient, α, can be computed using $\alpha = 1-(K/K_s)$, where K_s is the bulk modulus of solid grains;

β_m is defined as $\beta_m = \alpha\beta_s + (\beta_f - \beta_s)n$, where β_f is thermal expansion coefficient of the fluid and n is porosity; κ is defined as $\kappa = k/\mu$, where k is dynamic permeability and μ is fluid viscosity.

It should be noted that for most rocks, heating/cooling produces thermal stresses and changes pore pressure, but stress and pressure changes do not significantly alter the temperature field (Wang, 2000) so that they are not coupled to the diffusion equation for the temperature.

A few analytical procedures have been developed and used to solve geomechanics problems of interest involving coupled thermal and poromechanical problems (e.g., Ghassemi and Diek, 2002; Wong and Papamichos, 1994). However, many problems formulated within the framework of poro-thermoelasticity are not amenable to analytical treatment and need to be solved numerically. The boundary element method (BEM) or the boundary integral equation formulation has been used extensively for the poroelastic and thermoelastic problems (e.g., Cheng, *et. al.*, 2001; Ghassemi, *et. al.*, 2001). The advantage of the method is that it reduces the problem dimensionality by one thereby reducing the computational efforts significantly.

The indirect BEM has two sub-formulations, namely, the *displacement discontinuity* (DD) method and the *fictitious stress* (FS) method. The former is particularly useful for modeling fractures and fracture propagation. This paper is concerned with wellbore failure and fracture initiation using a classical approach and thus its focus is the fictitious stress method. And although DD and FS methods have totally different physical meanings, they are almost identical in structure and with some modifications the following discussion can also be applied to the DD method.

Poro-thermoelastic Fictitious Stress Method

The FS method is based on the fundamental solutions for a point force, point fluid source, and point heat source applied within an infinite porothermoelastic solid. Fictitious forces, fluid sources, and heat sources are distributed over the boundary Γ of the problem domain and the principle of superposition is used to add their effects such that the boundary conditions of the problem are satisfied. This requires both spatial integration along the boundary Γ and temporal integration along time because of the time-dependent nature of the heat/fluid diffusion and deformation processes.

Suppose the problem boundary, Γ (e.g., the borehole wall) is divided into N straight elements (Figure1) and the time at which a solution is desired, t, is divided into M time steps. Then, at a given time the shear stress (σ_s), normal stresses (σ_n), pore pressure (p), and temperature (T) at the midpoint of the ith element can be expressed in terms of the stresses, pore pressure, and temperature induced by the continuous fictitious forces and fluid/heat sources applied on all other elements (j) over time:

$$\sigma_s^i = \sum_{t\neq 1}^{M}\sum_{j=1}^{N}\left\{\sigma_{ss}^{ij}F_s^j + \sigma_{sn}^{ij}F_n^j + \sigma_{sf}^{ij}\phi^j + \sigma_{sh}^{ij}\varphi^j\right\} \qquad i=1 \text{ to } N \quad (4)$$

$$\sigma_n^i = \sum_{t\neq 1}^{M}\sum_{j=1}^{N}\left\{\sigma_{ns}^{ij}F_s^j + \sigma_{nn}^{ij}F_n^j + \sigma_{nf}^{ij}\phi^j + \sigma_{nh}^{ij}\varphi^j\right\} \qquad i=1 \text{ to } N \quad (5)$$

$$p^i = \sum_{t\neq 1}^{M}\sum_{j=1}^{N}\left\{p_s^{ij}F_s^j + p_n^{ij}F_n^j + p_f^{ij}\phi^j + p_h^{ij}\varphi^j\right\} \qquad i=1 \text{ to } N \quad (6)$$

$$T^i = \sum_{t\neq 1}^{M}\sum_{j=1}^{N}\left\{T_h^{ij}\varphi^j\right\} \qquad i=1 \text{ to } N \quad (7)$$

where F_s^j, F_n^j, ϕ^j, and φ^j are strengths of shear fictitious force, normal fictitious force, fluid source, and heat source at the jth element, respectively. The terms σ_{ss}^{ij}, etc. are the boundary influence coefficients. The coefficient σ_{ss}^{ij}, for example, gives the shear stress at time t at the midpoint of the ith segment due to a constant unit shear fictitious force (F_s) applied to the jth segment at time τ. σ_{sf}^{ij} is the shear stress due to a constant unit fluid source strength (ϕ) at the jth segment. And σ_{sh}^{ij} is the shear stress due to a constant unit heat source of strength (φ) at the jth segment. The coefficients for stress, pore pressure, and temperature due to a constant distribution of sources and forces on a straight element are obtained by integration of the fundamental solutions in space and time.

The proposed coupled poro-thermoelastic BEM is based on two kinds of fundamental solutions (i) the pore pressure and stresses induced by a unit continuous fluid point source and by a unit continuous point force in poroelastic media (e.g., Curren and Carvalho 1987); (ii) the temperature, pore pressure, and stresses induced by a unit continuous heat point source in a poroelastic medium. The latter are given by the following expressions (Berchenko, 1998):

$$T = \frac{1}{4\pi\kappa^*}Ei(\xi^2) \quad (8)$$

$$p = \frac{\beta_0}{4\pi\kappa^* S(1-\omega^2)}\left[Ei(\xi^2) - Ei(\xi^2/\omega^2)\right] \qquad \text{for } \omega^2 \neq 1 \quad (9)$$

$$p = \frac{\beta_0}{4\pi\kappa^* S}e^{-\xi^2} \qquad \text{for } \omega^2 = 1 \quad (10)$$

$$\sigma_{ij} = \frac{\eta\beta_0}{4\pi\kappa^* S(1-\omega^2)}\left[\lambda F\left(x_i;x_j;\xi^2\right) - F\left(x_i;x_j;\frac{\xi^2}{\omega^2}\right)\right] \text{ for } \omega^2 \neq 1 \quad (11)$$

$$\sigma_{ij} = \frac{\eta\beta_0}{4\pi\kappa^* S}\left[\lambda_1 F\left(x_i;x_j;\xi^2\right) - F'\left(x_i;x_j;\xi^2\right)\right] \qquad \text{for } \omega^2 = 1 \quad (12)$$

In above equations, ξ^2 is given by $\xi^2 = \frac{r^2}{4c^f t} = \frac{x_i^2 + x_j^2}{4c^f t}$; κ^* is thermal conductivity; $\omega^2 = \frac{c^f}{c^T}$, where c^f is hydraulic diffusivity. Other constants are defined as: $\beta_0 = \beta_m - \frac{3\alpha\beta_s K}{3K+4G}$; $S = \frac{1}{M} + \frac{3\alpha^2}{3K+4G}$; $\eta = \frac{3\alpha G}{3K+4G}$; $\lambda_1 = \frac{K\beta}{\alpha\gamma}$; $\lambda = 1 + (1-\omega^2)\lambda_1$.

Functions used in above equations are:

$$Ei(x) = \int_x^\infty \frac{e^{-z}}{z}dz \qquad \text{(exponential integral function)}$$

$$F(x_i;x_j;\xi^2)=\left(\delta_{ij}-\frac{2x_ix_j}{r^2}\right)\left[\frac{1-e^{-\xi^2}}{\xi^2}\right]-Ei(\xi^2)\delta_{ij}$$

$$F'(x_i;x_j;\xi^2)=\xi^2\frac{\partial F(x_i;x_j;\xi^2)}{\partial\xi}=$$

$$-\left(\delta_{ij}-\frac{2x_ix_j}{r^2}\right)\left[\frac{1-e^{-\xi^2}}{\xi^2}\right]-2\left(\delta_{ij}-\frac{x_ix_j}{r^2}\right)e^{-\xi^2}$$

All influence coefficients are obtained by spatial integration of the fundamental solutions assuming a particular distribution of forces and source along an element. In the present formulation, it is assumed that the distribution of forces and sources are constant in space and time over an element. Also, it is assumed that the boundary elements are straight segments with the collocation points located at the center of each element. The space integrals are performed analytically and numerically. The time integration is performed using a time marching approach that solves the problem at the end of a time step and keeps a solution history (Banerjee and Butterfield, 1981) for the next step. That is, the time integration is carried out in a convolution sense, so that no internal discretization would be necessary. This process yields a system of linear algebraic equations (4-7) that can be solved at each time step for the increment of unknown heat sources, fluid sources, and fictitious forces. As mentioned previously, the influence of deformation and pressure variations on the temperature field can be neglected. Therefore, the temperature field and heat flux are calculated independently.

Examples

Consider a borehole with radius $R = 0.1m$ in a reservoir at a temperature of 200°C. The wellbore wall is suddenly cooled by water and maintained at 0°C. For clarity of presentation and investigation of the role of temperature, only induced stress and pore pressure are studied. Thus, pore pressure and stress loadings are not considered, meaning that the far field pore pressure and stresses are considered to be zero. Due to symmetry only a quarter of the wellbore is modeled and 10 elements are used to approximate one-quarter of the circular boundary. Number of time steps is 10 for each computation and the time step length, Δt, is adjusted accordingly. The input parameters are shown in Table 1.

Table 1. Input Parameters.

E	Modulus of elasticity	$2.06*10^4$	MPa
ν	Poisson's ratio	0.20	
ν_u	Undrained Poisson's ratio	0.31	
K_s	Solid bulk modulus	$4.82*10^4$	Mpa
K_f	Fluid bulk modulus	$2.50*10^3$	Mpa
c^T	Thermal diffusivity	$1.60*10^{-6}$	m^2/sec
C	Heat capacity	$1.169*10^6$	Joule/(kg*°C)
β_s	Solid thermal expansivity	$1.80*10^{-5}$	m/°C
β_f	Fluid thermal expansivity	$3.00*10^{-4}$	m/°C
η	Porosity	0.143	
γ_f	Unit weight of fluid	$9.8*10^3$	kg/m^3
k	Dynamic permeability	$7.66*10^{-8}$	m/sec
B	Skempton's constant	0.551	
M	Biot modulus	$1.427*10^4$	Mpa
μ	Fluid viscosity	$3.0*10^{-4}$	kg/(m*sec^2)

Figures 1-4 illustrate the profiles of temperature, induced pore pressure, induced tangential stress, and radial stress around the wellbore. Analytical results are also shown for comparison. As can be observed, the numerical results are in good agreement with the analytic solution. This demonstrates the validity of this numerical approach for poro-thermoelastic problems.

Figure 1 shows the transient temperature distribution; it is typical of a conductive heat transfer situation. The formation is gradually cooled off when the borehole temperature is suddenly reduced to a constant value. Figure 2 is the distribution of induced pore pressure. One can see that a significant pressure drop is generated near the borehole at early times. With time,

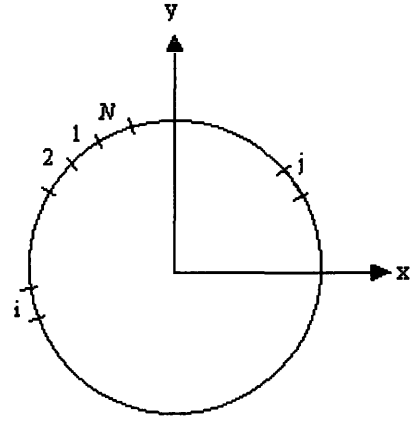

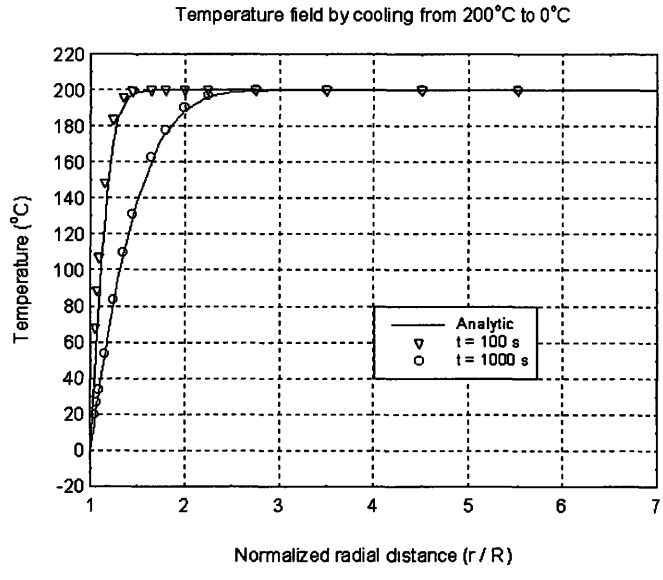

Figure 2. Distribution of temperature around the borehole.

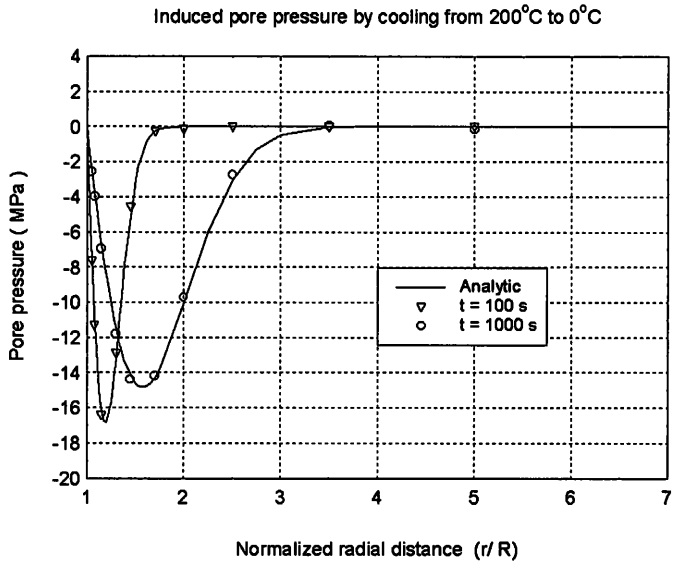

Figure 3. Distribution of induced pore pressure around the borehole.

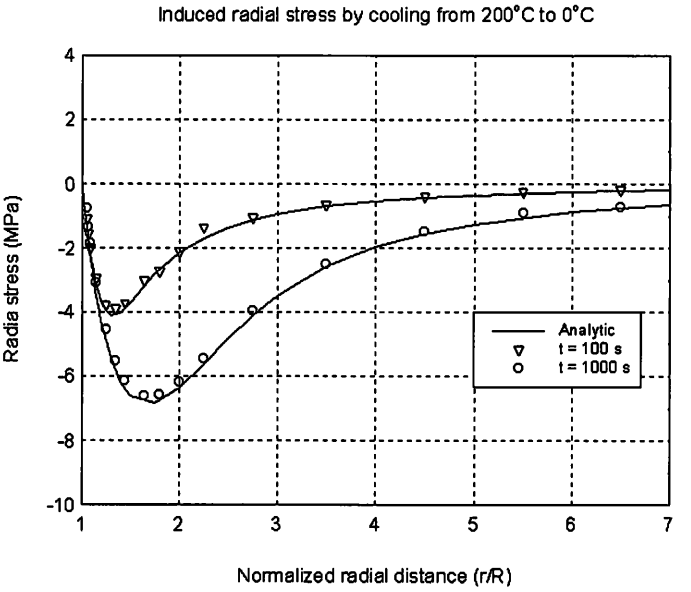

Figure 5. Distribution of induced radial stress around the borehole.

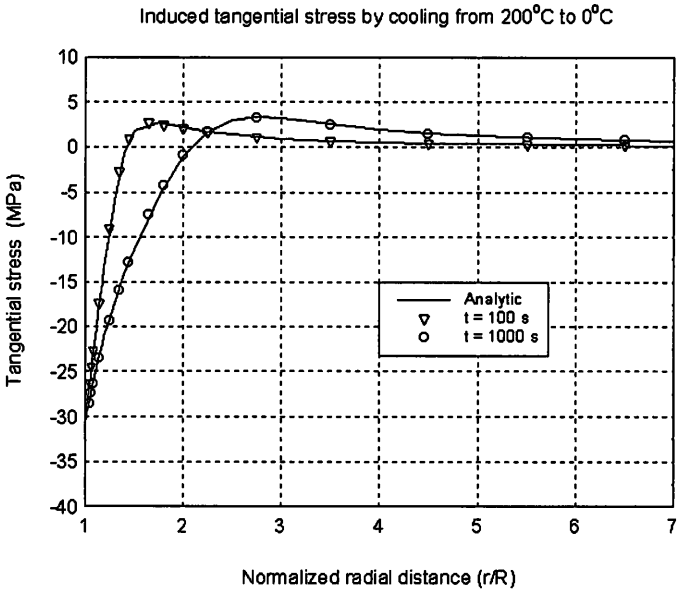

Figure 4. Distribution of induced tangential stress around the borehole.

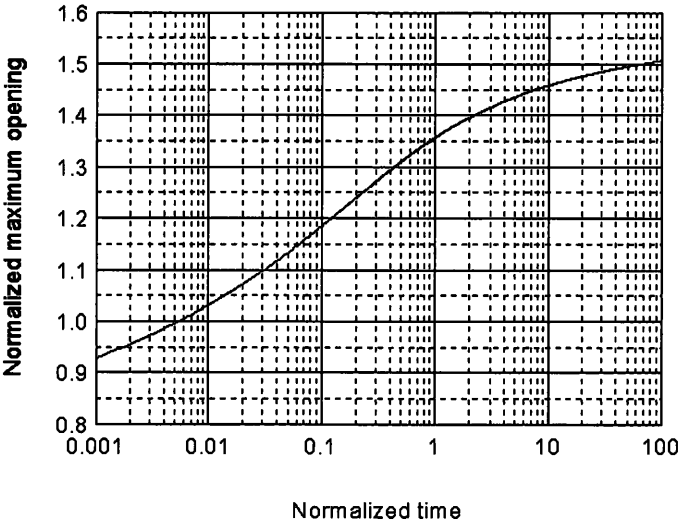

Figure 6. Maximum opening of a suddenly pressurized and cooled crack.

the pore pressure will gradually recover its original state. Figure 3 presents the thermally induced tangential stress. With cooling, a significant tangential tensile stress is induced around the wellbore. This is caused by the tendency of the rock to shrink near the borehole wall. Away from the borehole wall, the magnitude of the induced tensile stress decreases and at some point inside the formation changes its sign, turning into a compressive stress. This is because the shrinkage of the material at the inner face of the borehole geometry, due to cooling, tends to pull on the outer rock thus inducing a compressive stress. The compressive zone fades away with distance and gradually moves away from the borehole. Figure 4 illustrates the thermally induced radial stress. A significant radial tensile stress peak is produced inside the formation. At later times, the tensile stress zone moves inside the formation while the magnitude of the "peak" increases.

From above, one can expect that the potential for fracturing of the wellbore wall in shear increases. This is because the maximum difference between the tangential and radial stresses occurs at the wellbore wall. As for tensile failure, the induced tangential stresses will lower the pressure necessary to fracture the rock in tension. Also, the fracturing will always initiate from the wellbore boundary because the maximum tensile stress occurs there. Moreover, the extent of the tensile stress zone that develops inside the formation increases with time facilitating a time-delayed fracture development.

Table 2. Input data for the fracture problem.

Far Field Condition	
Stresses	0.0 MPa
Temperature	200 °C
Boundary Condition	
Normal Stress	82.73 MPa
Temperature	0°C
Modeling Condition	
Crack dimension	(-5.0, 0.0) to (5.0, 0.0)
Total number of elements	15
Symmetric with Y axis ?	No
Time step length Δt	360s, 3600s, 14400s
Number of time steps	2000

Table 3. Other Relevant Input Parameters.

G	Shear modulus	$8.273*10^4$	MPa
ν	Poisson's ratio	0.1	
c^T	Thermal diffusivity	$1.39*10^{-5}$	m^2/sec
β_s	Thermal expansivity	$1.20*10^{-5}$	m/°C
C	Heat Capacity	$1.60*10^6$	Joule/(kg*°C)

Efforts are underway to develop a porothermoelastic DD program also. The coupling between temperature and fluid diffusion has not been implemented at the present time. Thus, the current version of the DD model is purely thermoelastic. Nevertheless, it is used here to underline the significance of thermal stresses in fracture propagation. For the purpose of illustration, consider a uniformly cooled and pressurized crack in a rock mass. The length of the crack is 10.0m and the input parameters are shown in Tables 2 and 3.

The normalized maximum opening, $D^*= GD/(PL)$, (at the center of the crack) vs. normalized time, $t^* = c^T t / L^2$, is plotted in Figure 5. Note that $D(t)$ is the opening at midpoint of the crack and G is the shear modulus, P is normal stress at crack face, and L is the half-length of the crack. As can be observed in the figure, the crack opens as a result of cooling and pressurization. The fracture response is transient and the crack opening gradually increases due to the shrinkage of the rock. The opening increases and approaches a maximum value asymptotically.

The results presented herein illustrate the importance of the role of temperature in hydraulic fracture initiation and propagation. Cooling of the wellbore can lead to fracturing; it also increases the stress intensity at the fracture tip leading to crack growth. The combined effects of fluid pressure and temperature on fracture opening and propagation will be examined in the future.

Acknowledgement

The financial support of the US Department of Energy (DE-FG07-99ID13855) is gratefully acknowledged. Also acknowledged is the financial support of North Dakota EPSCoR through NSF grant #EPS-9874802 and the Office of Research and Program Development of the University of North Dakota.

Reference

Banerjee, P.K., and Butterfield, R. 1981. *Boundary element methods in engineering science*, McGraw-Hill, London, pp. 452 .

Berchenko, I. 1998. Thermal Loading of Saturated Rock Mass: Field Experiment and Modeling Using Thermoporoelastic Singular Solutions. Ph.D. Dissertation, University of Minnesota.

Biot, M.A. 1941. General theory of three-dimensional consolidation, *J. Appl. Phys.*, 26, pp. 182-185.

Cheng, A. H.-D., Ghassemi, A., and Detournay, E. 2001. A two-dimensional solution for heat extraction from a fracture in hot dry rock. *Int. J. Numerical & Analytical Methods in Geomech. Int. J. Numerical & Analytical Methods in Geomech.*, 25, 1327-1338.

Curran, J.H., and Carvalho, J.L. 1987. A displacement discontinuity model for fluid-saturated porous media, Proc Sixth Congress of the ISRM, Montreal, 1, pp. 73-78.

Ghassemi, A., Cheng, A. H.-D., Diek, A., and Roegiers, J.-C. 2001. A complete plane- strain fictitious stress boundary element method for poroelastic media. *J. Eng. Anal. Boundary Elements,V. 25, No. 1, p. 41-48.*

Norris, A.N. 1992. On the correspondence between poroelasticity and thermoelasticity, *J. Appl. Phys.*, 71, pp. 1138-1141.

Palciauskas V.V., Domenico P.A. 1982. Characterization of drained and undrained response of thermally loaded repository rocks, *Water Resour. Res.*, 18, pp. 281-290.

Rice, J. R. and Cleary, M. P. 1976. Some basis stress diffusion solutions for fluid-saturated elastic porous media with compressible constituents, *Reviews of Geophysics and Space Physics.* 14, pp. 227-241.

Smith, D.W. and Booker, J.R. 1993. Green's functions for a fully coupled thermoporoelastic material. *Int. J. Num. Anal. Methods Geomech.*, 17, pp. 139-163.

Wang, H.F. 2000. *Theory of Linear Poroelasticity with Applications to Geomechanics and Hydrogeology*, Princeton University Press, Princeton, pp. 240.